Transportation Research Part C 104 (2019) 53–65

Contents lists available at ScienceDirect

Transportation Research Part C

journal homepage: www.elsevier.com/locate/trc

Developing an actuated signal control strategy to improve the operations of contraflow left-turn lane design at signalized intersections

Jiaming Wu[a], Pan Liu[a,*], Xiao Qin[b], Huaguo Zhou[c], Zhao Yang[d]

[a] Jiangsu Key Laboratory of Urban ITS, Southeast University, Jiangsu Province Collaborative Innovation Center of Modern Urban Traffic Technologies, Si Pai Lou #2, Nanjing 210096, China

[b] Department of Civil and Environmental Engineering, University of Wisconsin-Milwaukee, NWQ4414, P.O. Box 784, Milwaukee, WI 53201, United States

[c] Department of Civil Engineering, Auburn University, 238 Harbert Engineering Center, Auburn, AL 36849-5337, United States

[d] National Key Laboratory of Air Traffic Flow Management, College of Civil Aviation, Nanjing University of Aeronautics and Astronautics, Jiangjun Road No. 29, Nanjing 211106, China

ARTICLE INFO

Keywords:
Contraflow left-turn lane
Unconventional design
Actuated signal control
Shock wave
Signalized intersections

ABSTRACT

Contraflow left-turn lane (CLL) design has been increasingly used in China to help relieve traffic congestion associated with left-turning vehicles at signalized intersections. With the CLL design, one or multiple left-turn lanes are setup in the opposing through lanes adjacent to the median. The basic idea of the CLL design is to provide additional capacity to left-turning vehicles by making use of the opposing through lanes. The primary objective of the present study was to propose an actuated signal control strategy to improve the operations of the CLL design at signalized intersections. The proposed control strategy introduced an extra stage between the pre-signal and the main signal at the signalized intersection with the CLL design. Two detectors were installed: one at the upstream median opening and the other at the contraflow lane. A procedure was proposed for optimizing the distance between the upstream median opening and the main signal, such that the discharge rate of the left-turning vehicles and the utilization rate of the contraflow lane can be maximized. Simulation experiments were conducted to compare the performance of the proposed actuated control strategy versus the fixed time control strategy. The results show that the proposed design concept outperforms the fixed time control strategy in increasing capacity and reducing delay for left-turning vehicles.

1. Introduction

Signalized intersections are main bottlenecks. Previous researchers have proposed numerous unconventional design concepts to relieve traffic congestion at signalized intersections. These unconventional design concepts include median U-turns, continuous flow design, left-turn waiting area design, outside left-turn lane design, tandem design and more recently, the contraflow left-turn lane (CLL) design (Hummer, 1998; Liu et al., 2008, 2011; Xuan et al., 2011; Yang et al., 2012; El Esawey and Sayed, 2013; Yang et al., 2013; Zhao et al., 2013; Bie and Liu, 2014; Krause et al., 2014; Dong et al., 2016; Guler et al., 2016; Kozey et al., 2016; Wu et al.,

* Corresponding author.
E-mail addresses: wujiaming123456@yeah.net (J. Wu), liupan@seu.edu.cn (P. Liu), qinx@uwm.edu (X. Qin), hhz0001@auburn.edu (H. Zhou), yangzhao@nuaa.edu.cn (Z. Yang).

https://doi.org/10.1016/j.trc.2019.04.028
Received 7 September 2017; Received in revised form 9 March 2019; Accepted 29 April 2019
Available online 27 May 2019

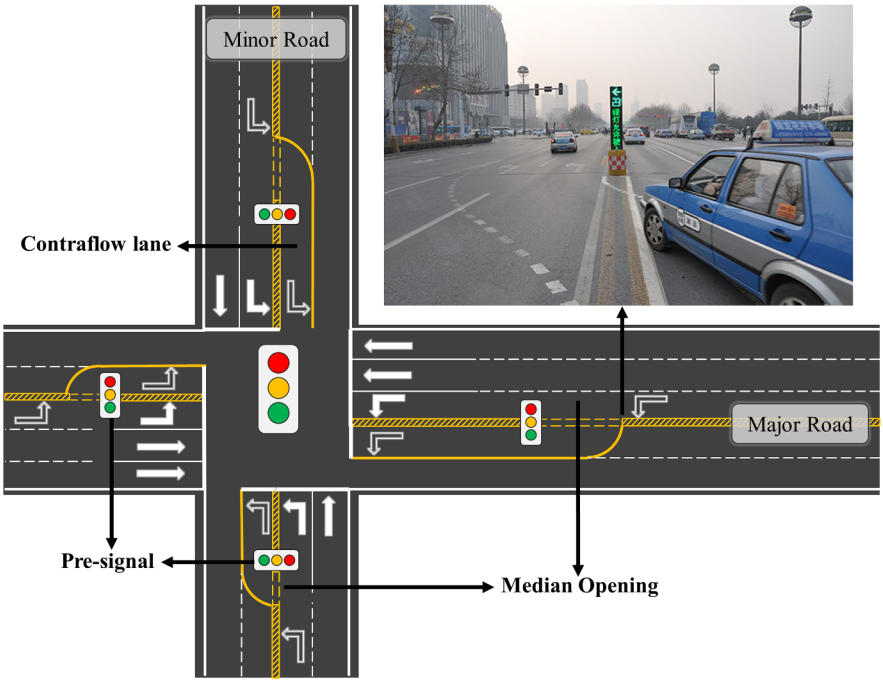

Fig. 1. Geometric layout of contraflow left-turn lane design.

2016; Yang and Cheng, 2017; Yang and Shi, 2017; Zhao et al., 2018). As for the CLL design, one or multiple contraflow left-turn lanes are deployed in the opposing through lanes adjacent to the median. The basic idea of the design concept is to provide additional capacity to left-turning vehicles by making use of the opposing through lanes dynamically.

A typical geometric layout of the CLL design at a signalized intersection is shown in Fig. 1. On each approach, a median opening is installed upstream of the stop line at the main signal. A pre-signal with the same signal cycle as the main signal is setup at the median opening to control the vehicles entering the contraflow lane. The CLL design can be deployed to one or multiple legs of a signalized intersection. If the CLL is deployed to one leg only, it will not affect the signal timing planning and geometric design of the other three legs. Thus, the use of CLL design could be quite flexible, and its applicability depends on the geometric design characteristics and traffic conditions at signalized intersections. In China, the CLL design was deployed at five signalized intersections in the city of Handan in 2014 and has been expanded to more than fifty signalized intersections in twelve cities during the past three years.

Fig. 2 depicts the signal timing plan for the CLL design at a four-leg signalized intersection with a stage-based scheme. Note that in Fig. 2 the CLL design is applied to four legs of the intersection. For convenience, the right-turn movements and pedestrians are excluded because they do not significantly influence the operations of the CLL design. Therefore, there is only one movement in each phase, and both movements and phases are denoted by the green squares in Fig. 2. In stage one, the through movements on the minor road are starting to be discharged (movement 4 and 8 in Fig. 2). After a while, the pre-signals on the major road turn green and the left-turning vehicles queuing upstream of the median openings are starting to enter the contraflow lanes through the median openings (movement 9 and 12). In stage two, the left-turning vehicles in both conventional and contraflow lanes are starting to be discharged together (movement 1 and 5). In this stage, the pre-signals on the major road turn red, and the entrance into contraflow lanes is prohibited. The purpose is to guarantee that vehicles in the contraflow lanes can be fully discharged during stage two. The following two stages are similar to the first two stages mentioned above. A field video is provided to help readers better understand the design concept (see: https://youtu.be/xb5cvAAbuIQ). Note that the use of CLL design requires a leading protected left-turn phase and the left-turn movements should follow the through movement on the crossing street.

The idea of using pre-signals at signalized intersections is not new. Xuan et al. proposed an unconventional left-turn treatment called “tandem” intersection design. Two stop lines were deployed at a signalized intersection, and the area between these two stop lines is called the “sorting area”. The lanes in the sorting area are jointly and dynamically used by both left-turning and through vehicles. A pre-signal is installed upstream of the main signal to allocate green time to left-turning and through vehicles alternatively. The pre-signal starts its cycle by giving green time to the left-turn movement, allowing the left-turning vehicles to enter the sorting area when the main signal turns red. Then, the pre-signal allows the through vehicles to enter the sorting area, lining up behind the left-turning vehicles. With the tandem design, both left-turning and through vehicles can make use of more lanes than those at conventional signalized intersections, resulting in increased capacity (Xuan et al., 2011).

Several researchers have evaluated the safety and operational performance of the CLL design. Zhao et al. employed a lane-based algorithm to optimize the CLL design. They conducted simulation-based analyses using a VISSIM simulation model to evaluate the effects of the CLL design. The results suggested that the CLL design increases the capacity of signalized intersections (Zhao et al., 2013; Wong and Wong, 2003). Wu et al. evaluated the operational performance of the CLL design with the field data collected from

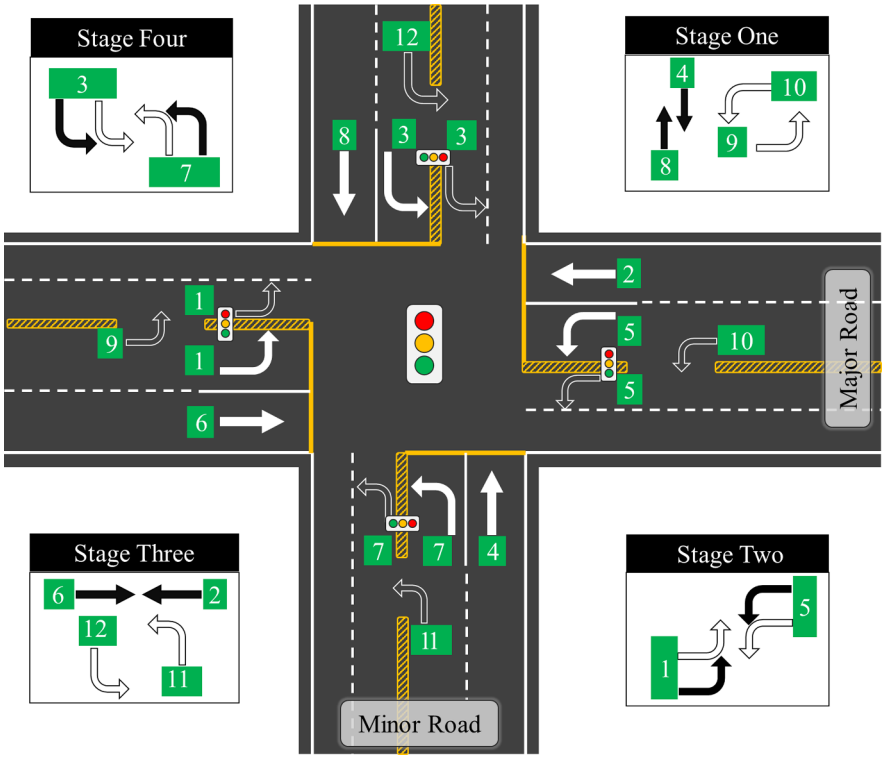

Fig. 2. Signal control plan for the main and pre-signals at the signalized intersection with the CLL design.

five signalized intersections in Handan, China. The authors developed analytical models to calculate the capacity and delay associated with the left-turn movements at the selected intersections with the CLL design. They found that the CLL design improves the capacity of left-turning vehicles at signalized intersections, and the capacity gains mainly depend on the number of left-turning vehicles that are discharged through the contraflow lanes. Therefore, the capacity gains associated with the CLL design could be quite stochastic because the usage of contraflow lanes is heavily affected by the arrival pattern of left-turning vehicles. Wu et al. also proposed a procedure for optimizing the location of the upstream median opening and the green interval of the pre-signal, given the signal timing plan of the main signal. The authors compared the operational performance of the conventional design, the tandem design, and the proposed contraflow left-turn lane design through traffic simulations. The results indicated that the CLL design generates less delay to both through and left-turn movements than the conventional and tandem design do (Wu et al., 2016).

Despite the benefits that have been demonstrated by previous studies, the CLL design may suffer from several limitations: (*a*) vehicles that cannot be fully discharged from the contraflow lanes may be exposed to the risks of head-on collisions with the through vehicles in the opposing direction, leading to safety concerns at signalized intersections; (*b*) the storage capacity of CLLs sometimes cannot be fully used mainly because of the stochastic arrival pattern of left-turning vehicles; and (*c*) the green-time duration of the pre-signal is constrained by the green-time duration of the through movement on the crossing street, resulting in limited capacity gains achieved by the CLL design.

So far all the signalized intersections with the CLL design in China used a fixed time signal control system. The primary objective of the present study was to propose an actuated signal control strategy to improve the operations of the CLL design at signalized intersections. We expect that with the proposed actuated signal control strategy the limitations associated with the fixed time CLL design can be addressed, and the operations of the CLL design can be improved. The rest of the paper is organized as follows. First, the data sources and field data collection procedure are presented. The paper then elaborates the proposed actuated signal control strategy and discusses the design optimization procedure, followed by a discussion on the comparative analysis results. The conclusion and discussion of research findings are included in the last section.

2. Field data collection

The authors conducted field data collection at six approaches at five signalized intersections in Handan, China. The following criteria were applied for site selection: (*a*) the selected intersection should be a four-leg intersection, and at least one of the approaches should be deployed with the CLL design; (*b*) for the selected approaches, there were no bus stations or roadside parking space within 100 m upstream and downstream of the stop lines; (*c*) the left-turn traffic demand should be high. More specifically, the average queue length for the left-turning vehicles should be greater than eight vehicles per cycle; and (*d*) the approach grade should be level. The characteristics of the selected sites are presented in Table 1.

Table 1
Characteristics of the selected signalized intersections.

Site	Intersection	D[a]	L[b] (m)	G^c_e (s)	g^d_e (s)	n^e_{cll}	n^f_{con}
1	Fudong RD & Lianfang RD	NB	50	25	35	2	1
2	Fuhe RD & Lianfang RD	WB	50	25	25	2	1
3	Fuhe RD & Lianfang RD	EB	50	25	25	2	1
4	Lianfang RD & Zhonghua RD	SB	43	15	15	1	1
5	Renmin RD & Fudong RD	SB	53	20	35	2	1
6	Renmin RD & Zhonghuabei RD	WB	50	25	23	1	1

[a] Direction of the approach where the contraflow left-turn lane was deployed.
[b] The length of the contraflow left-turn lanes.
[c] The green time for the left-turning vehicles at the main signals.
[d] The green time duration for the left-turning vehicles at the pre-signals.
[e] The number of contraflow left-turn lanes.
[f] The number of conventional left-turn lanes.

We collected three types of data at the selected sites: the geometric design characteristics, signal control features, and traffic flow data. The lane assignments and the distance between the stop lines and the pre-signals were directly measured in the field. A video camera was used for recording traffic flow and signal control data. The recorded videos were reviewed in the lab, and the following information was extracted from the recorded videos: (*a*) the cycle length, the stage sequence, and the green interval of the main signals; (*b*) the green interval of the pre-signals; and (c) the traffic flow data, including the discharge headways of the left-turning vehicles at the main signals from both the contraflow and the conventional left-turn lanes, the number of the left-turning vehicles in the contraflow left-turn lanes, and the number of the left-turning vehicles in the conventional left-turn lanes. The discharge headways of the left-turning vehicles at the main signals were measured using a stopwatch. While measuring discharge headways, the stop lines at the intersections were considered the reference lines. The first discharge headway was measured as the time interval between the initiation of the green signal and the time when the front wheel of the first left-turning vehicle crossed over the reference line. Other headways were measured as the time intervals between two successive left-turning vehicles crossing over the reference lines.

In total, 40 h of traffic data, which covered 783 cycles and 11,619 left-turning vehicles, were collected. The cycle length of the selected intersections ranged from 145 to 195 s. A parameter called utilization rate was defined and was used to evaluate the usage of the contraflow lanes. According to our previous study, the usage of contraflow lanes heavily affects the capacity gains achieved by the CLL design (Wu et al., 2016). The utilization rate was defined as the ratio of the actual number of vehicles that were discharged through the contraflow lanes to the ideal number of vehicles that should be discharged through the contraflow lanes. Theoretically, the ideal number of left-turning vehicles in the contraflow lanes may vary across different traffic conditions. More specifically, under low traffic-volume conditions, the ideal condition is that left-turning vehicles are evenly distributed across contraflow and conventional left-turn lanes, and the queue length in contraflow and conventional left-turn lanes are the same. Under heavy traffic-volume conditions, the ideal number of vehicles in contraflow lanes equals the storage capacity of contraflow lanes. Therefore, the utilization rate of CLL can be calculated as

$$Utlization\ Rate = \begin{cases} \frac{N_{CLL}(n_{cll}+n_{con})}{Qn_{cll}}, & if\ Q < \frac{L(n_{cll}+n_{con})}{L_{ave}} \\ \frac{N_{CLL}L_{ave}}{Ln_{cll}}, & if\ Q \geqslant \frac{L(n_{cll}+n_{con})}{L_{ave}} \end{cases} \quad (1)$$

where N_{CLL} denotes the actual number of vehicles that are discharged through contraflow lanes (veh); n_{cll} denotes the number of contraflow lanes; n_{con} denotes the number of conventional left-turn lanes; Q denotes the traffic demand per cycle (veh); L denotes the length of the contraflow lane (m); and L_{ave} denotes the average length of left-turning vehicles (m). The box-plots of the utilization rates observed at the selected sites are depicted in Fig. 3. As left-turn traffic demand increased, there was a general tendency that the utilization rate of contraflow lanes would also increase. However, the contraflow lanes were barely fully used even under heavy traffic-volume conditions. In addition, the utilization rate of the contraflow lanes was quite stochastic, especially under low and median traffic-volume conditions.

Of the 11,619 left-turning vehicles, 5045 were discharged through the contraflow lanes, while 6574 were discharged through the conventional left-turn lanes. The queue discharge patterns of the left-turning vehicles at the selected sites are displayed by plotting the average discharge headways for different queuing positions in Fig. 4. The queue discharge patterns did not display an easily identifiable saturation state, and the curves associated with the contraflow lanes were generally below the curves associated with the conventional left-turn lanes. The finding suggests that the average discharge headways in the contraflow lanes were smaller than those in the conventional lanes, and the difference in discharge headways was even larger at the end of the left-turn queues. The results are intuitive because field observations showed that the drivers in the contraflow lanes were concerned with getting discharged before the end of the left-turn stages, leading to compressed discharge headways at the end of left-turn queues. Note that the average discharge headways of the first vehicles at the selected sites were quite small, mainly due to the use of countdown signal timers (Liu et al., 2013).

Summary statistics of the discharge headways of the left-turning vehicles in both the contraflow and the conventional left-turn lanes are presented in Table 2. The observed discharge headways varied across different sites and different types of left-turn lanes. On

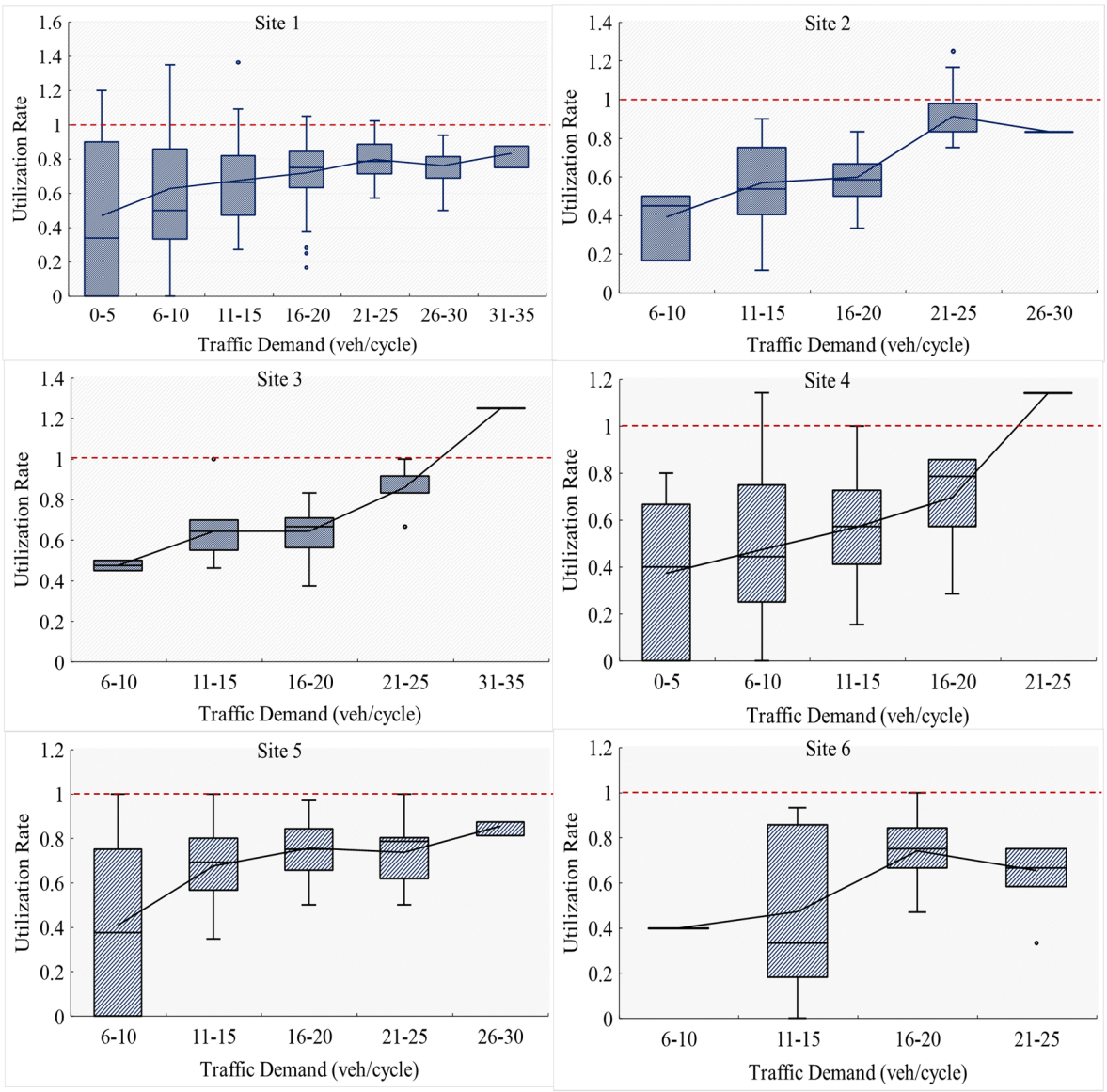

Fig. 3. The box-plots of the utilization rates of the contraflow lanes at the selected sites.

average, the discharge headways in the contraflow lanes varied from 0.98 to 9.57, with a mean of 2.65 s. The discharge headways in the conventional left-turn lanes varied from 0.86 to 10.81, with a mean of 2.78 s. When measuring the headways, we only took into account the left-turning vehicles that have stopped in the discharge lanes to distinguish random arrivals from queues. The observed large headways such as 9.57 and 10.81 s happened in very rare conditions which are possibly caused by drivers distractions. t-Tests were conducted to compare the average discharge headways in the conventional left-turn lanes and those in the contraflow lanes. The results suggest that the average discharge headways in the contraflow lanes were significantly smaller than those in the conventional lanes (p-value = 0.006).

The data in Table 2 suggest that the discharge headways were quite stochastic in both the conventional and the contraflow left-turn lanes. The maximum discharge headways observed at the selected sites varied from 6.55 to 10.81 s and were much larger than the mean discharge headways. Field observations showed that the extra-large discharge headways were mainly caused by abnormal driving behaviors such as hesitations and distractions. The great variance in the discharge headways of the left-turning vehicles increased the chance that the left-turning vehicles in the contraflow lanes failed to be discharged during the left-turn stages. This is probably the major safety concern associated with the CLL design. To address this concern, current practice is to use relatively short contraflow lanes. The limitations of this application are twofold: (*a*) short contraflow lanes reduce the capacity gains that can be achieved by the CLL design; (*b*) even with short contraflow lanes, it is still possible that the vehicles in the contraflow lanes cannot be fully discharged before the end of the left-turn phases. Of the 5045 vehicles observed at the selected contraflow lanes, 27 vehicles

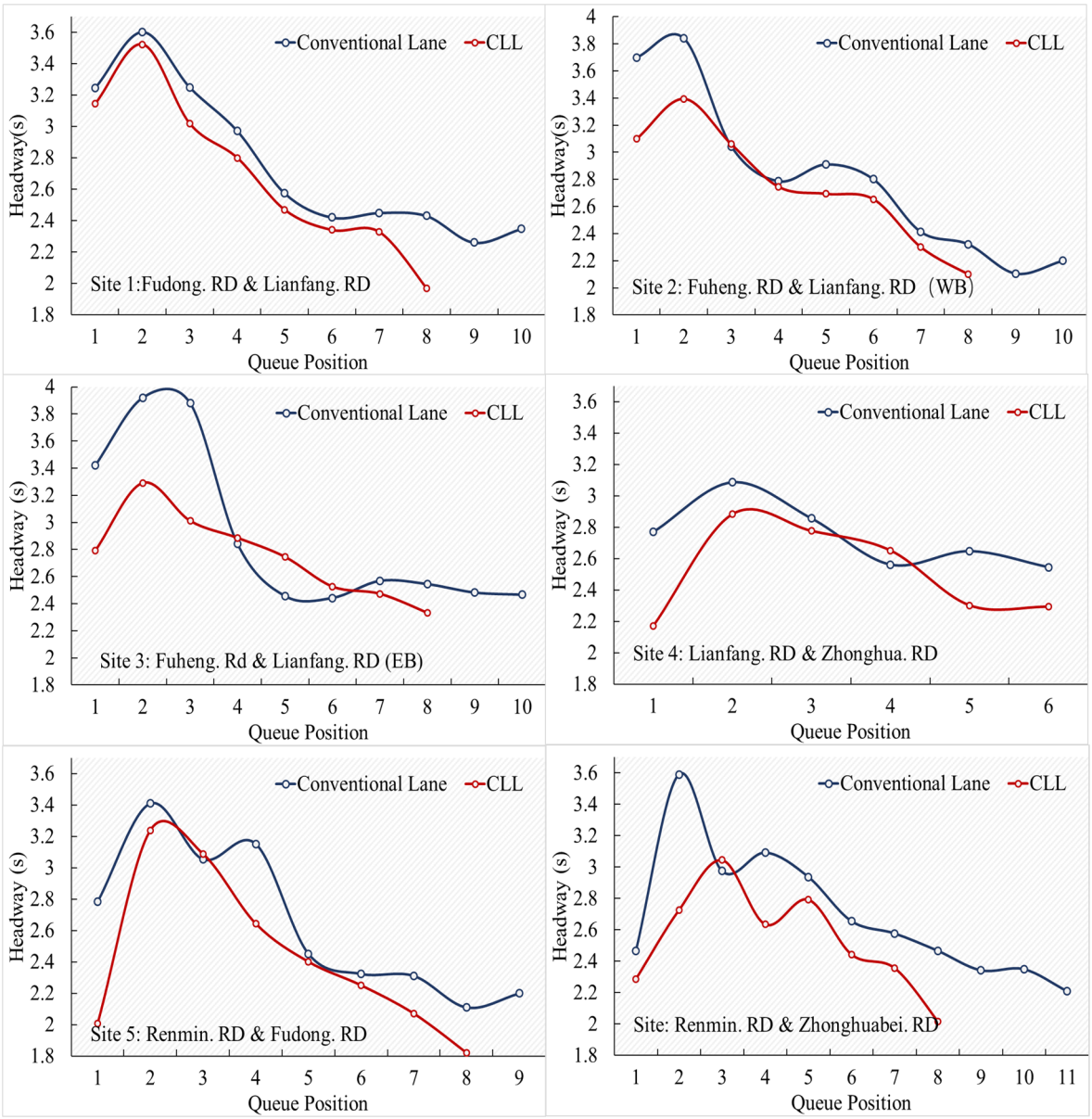

Fig. 4. Comparison of queue discharge patterns in contraflow and conventional left-turn lanes.

failed to get discharged before the end of the left-turn phases. Rather than staying in the contraflow lanes, all the 27 vehicles chose to run on the red light to avoid the potential conflicts with the opposing through vehicles.

3. Proposed actuated signal control strategy

Two major concerns need to be addressed to improve the operations of the CLL design at signalized intersections: (*a*) the CLL design uses a pre-signal to control the number of the left-turning vehicles that can enter the contraflow lanes. The left-turning vehicles can only enter the contraflow lanes during a pre-specified time window. Due to the random arrival patterns of left-turning vehicles, the contraflow lanes cannot be fully used, leading to limited capacity gains associated with the CLL design; and (*b*) the left-turning vehicles in the contraflow can only be discharged during a pre-specified time window, i.e., the left-turn stage of the main signals. Considering the large variation in queue discharge time, vehicles may fail to be discharged during the left-turn stage, leading to safety concerns.

In the present study, we proposed an actuated signal control strategy that aimed at addressing the concerns mentioned above. To simplify the problem, the present paper only focused on the most basic condition in which the CLL design was applied to one approach at a signalized intersection. We assumed that the other approaches have fixed green time duration. Therefore, the whole

Table 2
Summary statistics of the saturation headways of left-turning vehicles.

Site	Sample Size	Lane	Min.	Max.	Mean	Std. Deviations
1	2183	Conventional	0.93	10.81	3.02	1.14
	1861	Contraflow	1.05	9.57	2.91	1.01
2	568	Conventional	1.28	9.28	3.21	0.98
	471	Contraflow	1.09	8.26	2.77	0.74
3	919	Conventional	0.86	6.55	2.99	0.98
	766	Contraflow	1.36	9.16	2.55	0.89
4	777	Conventional	1.20	6.67	2.68	0.91
	289	Contraflow	1.09	5.39	2.56	0.75
5	1284	Conventional	1.00	8.30	2.78	0.92
	1168	Contraflow	0.98	8.39	2.70	0.93
6	842	Conventional	1.10	8.48	2.68	0.92
	490	Contraflow	1.10	7.31	2.57	0.89
Total	6574	Conventional	0.86	10.81	2.78	1.07
	5045	Contraflow	0.98	9.57	2.65	0.85

intersection is under semi-actuated control. The proposed strategy could be easily extended to full-actuated control plans under which the CLLs were deployed to multiple approaches. The detailed geometric design characteristics and signal control plan are shown in Fig. 5. Two sets of traffic detectors need to be installed to identify if there are vehicles waiting at the median opening and the contraflow lane, and their locations are depicted in Fig. 5. Both the main and the pre-signals are actuated signals that adjust the green time according to the left-turn traffic demand. Moreover, the proposed control strategy introduces an extra stage between the main and the pre-signals. The extra stage represents the time when both the main and pre-signals are green. With the extra stage, the time window through which the left-turning vehicles enter the contraflow lane is greatly extended, leading to an increased utilization rate of the contraflow lane. The stage-based signal control plan of the case illustrated in Fig. 5 is elaborated as follows:

Stage 1: the controller allocates green time to the left-turn movements from the minor street (movement 3 and 7);
Stage 2: the through vehicles (movement 4 and 8) from the minor street start to be discharged. After a few seconds, the pre-signal turns green and the left-turning vehicles (movement 9) are starting to advance into the contraflow lane through the median opening;
Stage 3: the left-turn phases in the main signals turn green and all the left-turning vehicles (movement 1 and 5) are starting to be discharged, including those in the contraflow and the conventional left-turn lanes. Meanwhile, the pre-signal remains green, and vehicles can still move into the contraflow lane (movement 9). The stage ends when either of the following conditions is satisfied: (a) the green time of the pre-signal reaches the pre-specified maximum value; and (b) the green time of the pre-signal is larger

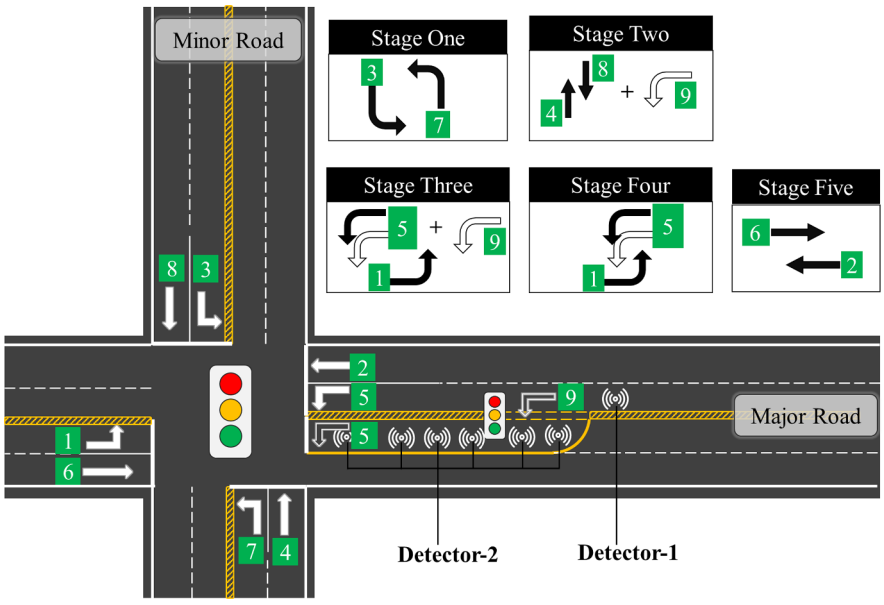

Fig. 5. A semi-actuated control example for the proposed CLL control strategy.

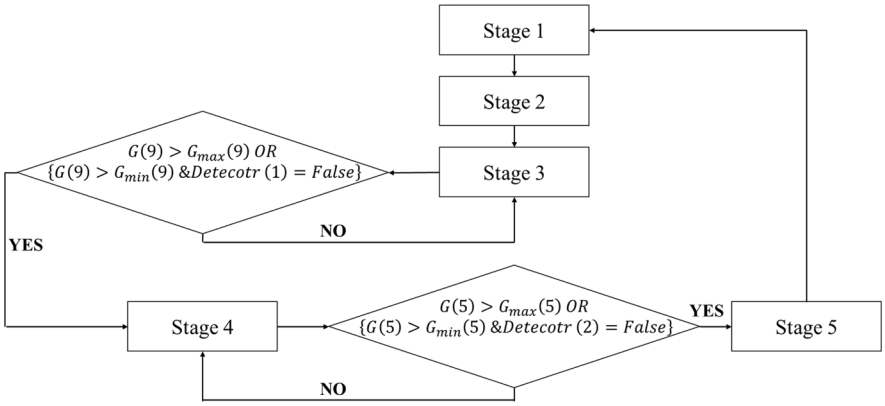

Fig. 6. Framework of the proposed signal control strategy.

than its minimum green time and no vehicles are detected by detector 1. Note that stage 3 is the extra stage mentioned above. When stage 3 ends, the pre-signal is turned off but the left-turn phases in the main signal still remain green;

Stage 4: the left-turning vehicles continue to be discharged (movement 1 and 5). The main signal will stay green as long as there are vehicles left in the contraflow lane, which can be detected by the detector 2. The stage 4 ends when either of the following conditions is satisfied: (a) the green time of the main signals is larger than its minimum value, and there are no vehicles left in the contraflow lane; and (b) the green time of the main signal reaches the pre-specified maximum value; and

Stage 5: the through vehicles (movement 2 and 6) from the major street start to be discharged, indicating the end of the cycle.

The control logic of the proposed semi-actuated control strategy is also depicted in Fig. 6 to help better understand the signal control plan.

3.1. The maximum and minimum green time duration

In actuated signal control systems, the maximum and minimum green time are critical parameters which define the interval of possible green time durations. In this section, the value of these two parameters for both the main signal and the pre-signal are discussed, respectively, considering the unique operations of the CLL design.

3.1.1. The main signal

The maximum green time duration of the main signal should be selected to ensure that vehicles in contraflow lanes can be fully discharged, considering the variations in discharge headways. In the proposed control strategy, the maximum green time for the left-turn movement at the main signal was used to address the extreme condition in which vehicles were trapped in the contraflow left-turn lane, which could be caused by mechanical failures or driver distractions. In this condition, without the constraint of the maximum green time, the left-turn phase in the main signal will always remain green and cause the collapse of the whole control system. The maximum green time is given by

$$G_{\max}(5) = T_s + N_{peak}(h + 3\sigma) \tag{2}$$

where $G_{max}(5)$ denotes the maximum green time for the left-turn movements in the main signal (s); T_s denotes the startup lost time of the left-turn queue in the contraflow lane, which equals 2.95 s according to the data at the selected sites (s); N_{peak} denotes the maximum number of the left-turning vehicles that are discharged in the contraflow lane during peak periods, and N_{peak} equals 10 vehicles per lane based on the data at the selected sites; h denotes the saturation headway of the left-turning vehicles in the contraflow lane, and h equals 2.65 s based on the data at the selected sites; and σ denotes the standard deviation of the saturation headway, and σ equals 0.85 s based on the data at the selected sites.

The function of Eq. (2) was developed based on the probability theory. The purpose was to ensure that the maximum green time was statistically long enough for a normal discharging process. According to the probability theory, $h + 3\sigma$ covers the vast majority of the possible discharge headways in the real world. For example, if the headway of left-turning vehicles follows a normal distribution, the probability that the average discharge headway is greater than $h + 3\sigma$ is smaller than 0.3%. Thus, the use of Eq. (2) ensures that vehicles will not fail to be discharged due to the stochastic nature of discharge headways. The maximum green time can only be reached in extreme conditions in which vehicles are trapped in the contraflow left-turn lane.

For the minimum green time duration of left-turn movements at the main signal, the CLL design doesn't actually introduce extra constraints. Conventionally, the minimum green time should be selected with specific conditions by considering drivers' expectancy, pedestrian needs, queue clearance and bicycle timing. We recommend that practitioners reference the Signal Timing Manual when deciding the minimum green time duration at the main signal (Urbanik et al., 2015).

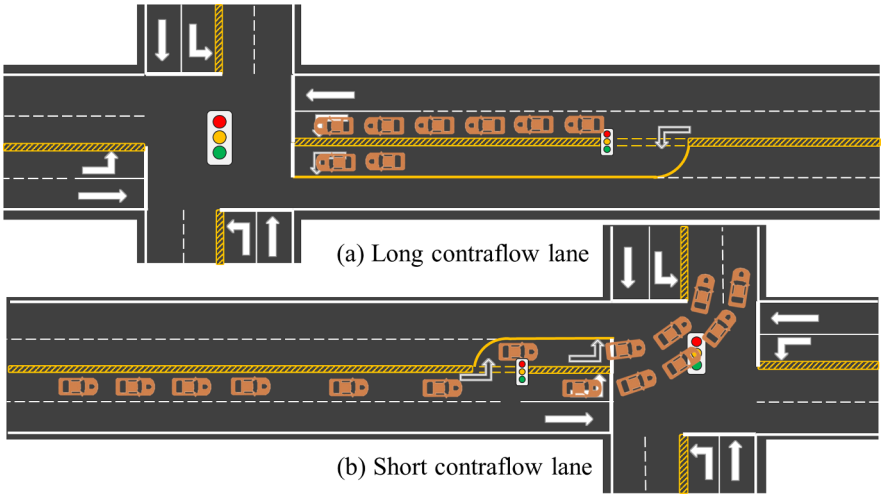

Fig. 7. Concerns with the use of long and short contraflow lanes.

3.1.2. The pre-signal

Considering the operational characteristics of the CLL design, the minimum green time duration at the pre-signal $G_{min}(9)$ can be set to be equal to the green time duration of through movements G(4) in the crossing road in Fig. 5. The maximum value of the pre-signal $G_{max}(9)$ can be set to be approximately equal to the sum of the green time duration for the through movement in the crossing road G(4) and the optimal green time duration of the left-turn movement. Note that in the real world the selection of maximum and minimum green time durations is quite subjective, and until recently, no widely accepted procedures or methods are available. In practice, the selection of maximum and minimum green time durations should consider both the operational characteristics of the CLL design, and other influence factors such as facility type.

4. Optimization of the CLL design

With the proposed semi-actuated control strategy, the location of the upstream median opening should be carefully selected such that the utilization rate of the contraflow lane can be maximized. Note that the location of the upstream median opening directly determines the length of the contraflow lane. The following two conditions need to be considered: (*a*) if the distance between the median opening and the main signal (*L*) is too long, the CLL design will be less efficient during off-peak periods, because only a few left-turning vehicles will use the contraflow lane (see Fig. 7(a)); while (*b*) if the L is too short, the left-turn lanes, including both the contraflow and conventional left-turn lanes, might be starved of traffic because there is only one lane for supplying left-turning vehicles, while multiple lanes for discharging them (Fig. 7(b)).

Considering the two conditions mentioned above, the optimization of the *L* can be considered a two-stage optimization problem. The first objective seeks to minimize the green time for the left-turn movements in the main signal during peak periods. The objective can be achieved when the left-turning vehicles that arrive at the intersection during the left-turn phase plus those queuing at the main signal are greater than or equal to the discharge capacity provided by both the contraflow and the conventional left-turn lanes. In this condition, all the left-turning vehicles can be discharged with the saturation flow rate. To achieve this objective, the *L* must be sufficiently long because it directly determines the storage capacity of the contraflow lane and, accordingly, the number of vehicles queuing at the main signal. When the first objective is satisfied, the second objective seeks to minimize the *L* such that the utilization rate of the contraflow lane can be improved during off-peak periods.

A graphical method based on the shock wave theory was used to solve the optimization problem. The shock wave theory was originally proposed by Lighthill-Whitham for modeling the dynamics of traffic flow (Lighthill and Whitham, 1955). Fig. 8 depicts the shock wave propagation and the corresponding fundamental diagram for a typical CLL design. Note that in the present study the shock wave analysis focuses on a single contraflow lane, which is bounded by the distance between the upstream median opening and the main signal (see Fig. 8). Assuming that the contraflow lane is fully occupied at the beginning, before the initiation of the left-turn stage in the main signal, the vehicles in the contraflow lane are in traffic state 2, which corresponds to the jam state in the fundamental diagram (see Fig. 8(c)). When the left-turn stage starts, vehicles in the contraflow lane start discharging at the saturation flow rate, and they are in traffic state 4, which corresponds to the capacity state in the fundamental diagram. The change from the traffic state 2 to the traffic state 4 generates a shock wave that propagates upstream, and the shock wave is denoted by the line *AC* in Fig. 8(b). When the shock wave moves to the rear end of the queue, all vehicles in the contraflow lane are in the traffic state 4, as shown in Fig. 8(b).

After that, vehicles will continue to enter the contraflow lane with an inflow rate that equals half of the saturation flow rate, because only half of the upstream left-turning vehicles will choose to use the contraflow lane (see Fig. 8(a)). The newly entered vehicles in the contraflow lane are in traffic state 3. A new shock wave, which is denoted by the line *CE*, is generated and keeps

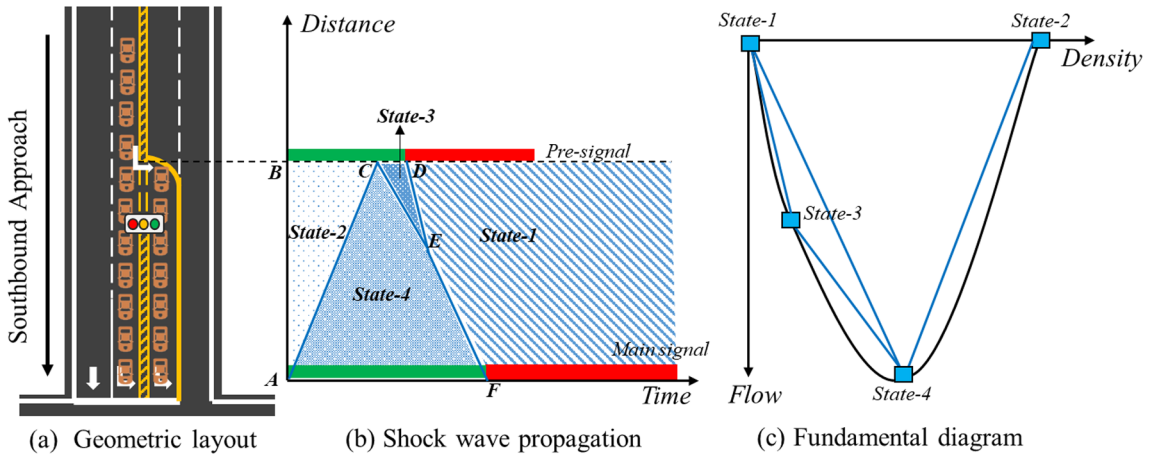

Fig. 8. Shock wave propagation and fundamental diagram for a typical CLL design.

transferring vehicles from the traffic state 4 to the traffic state 3. When the pre-signal is turned off, no vehicles can enter the contraflow lane. Another shock wave, which is denoted by the line *DE*, is generated, transferring vehicles from the traffic state 3 to traffic state 1. Note that the traffic state 1 is an empty state, which corresponds to the original point of the fundamental diagram. In Fig. 8(b), the shock wave *CE* and *DE* both move towards downstream and intersect at point *E* until all the vehicles are turned into the traffic state 4.

In practice, there are three different time-space diagrams, corresponding to long, short, and ideal contraflow lanes under the proposed semi-actuated control strategy (see Fig. 9(a)–(c)). Fig. 9 illustrates the traffic dynamics in the contraflow lane during the Stage Three as depicted in Fig. 5. When the length of the contraflow lane is too long, all the left-turning vehicles are transferred into the traffic state 4 before they reach the stop line (see Fig. 9(a)). In this condition, all the left-turning vehicles are discharged at the saturation flow rate, which satisfies the first objective of the optimization problem. However, the overlong contraflow lane will make the CLL design less efficient during off-peak periods, which does not meet the second optimization objective. If the length of the contraflow lane is too short, however, part of the left-turning vehicles will pass through the stop line when they are still in the traffic state 3. In other words, these vehicles will be discharged with a flow rate smaller than the saturation flow rate, leading to a longer queue discharge time (see Fig. 9(b)). Fig. 9(c) depicts the ideal condition in which all the left-turning vehicles are transferred into the traffic state 4 just when they reach the stop line. In this condition, all the left-turning vehicles are discharged at the saturation flow rate, and the length of the contraflow lane is also minimized. Note that the green time of the pre-signal shown in Fig. 9 depends on the number of vehicles that need to enter the contraflow lane during the Stage Three. Therefore, the green time of the pre-signal is different across Fig. 9(a)–(c).

Given the above discussions, the problem for optimizing the *L* can then be simplified and converted to the following computable simultaneous equations

$$G_{opt} = \frac{Q_p h}{n_{cll} + n_{con}} \tag{3}$$

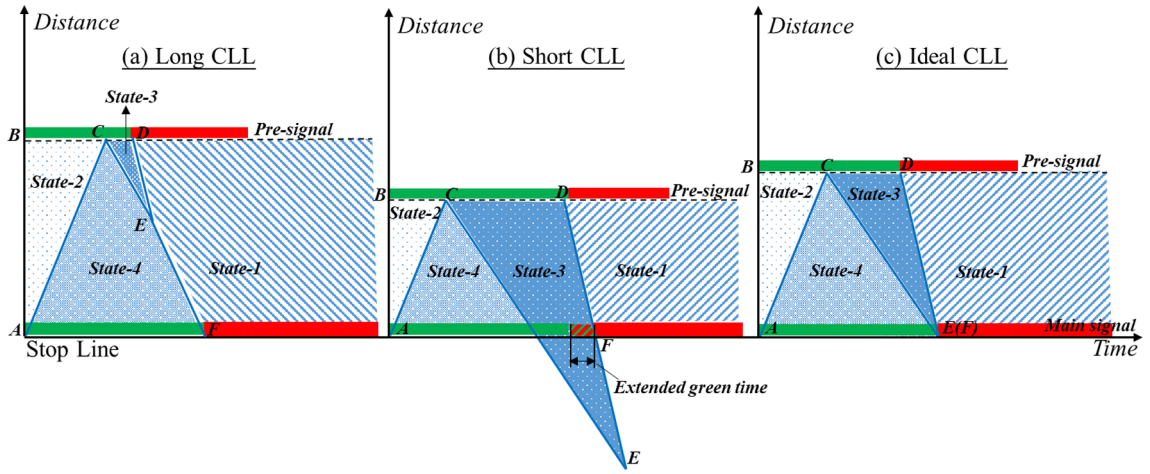

Fig. 9. The time-space diagrams for long, short and contraflow lanes.

$$T_{AC} = \left|\frac{L}{v_1}\right|; v_1 = \frac{q_4 - q_2}{3.6(k_4 - k_2)}$$

$$T_{CE} = \left|\frac{L}{v_2}\right|; v_2 = \frac{q_4 - q_3}{3.6(k_4 - k_3)}; q_3 = \frac{q_4 n_{con}}{n_{cll} + n_{con}}$$

$$G_{opt} = T_{AC} + T_{CE} \tag{6}$$

$$L = \frac{Q_p h}{3.6(n_{cll} + n_{con})} / \left(\frac{k_2 - k_4}{q_4 - q_2} + \frac{k_4 - k_3}{q_4 - q_3}\right) \tag{7}$$

where G_{opt} denotes the optimal green time of the left-turn movements at the main signal during peak periods, and can be calculated by assuming that all the left-turning vehicles are discharged at the saturation flow rate, and the queues in different left-turn lanes are all the same (s); Q_p denotes the left-turn traffic demand per cycle during peak periods (veh/cycle); q_i denotes the traffic flow rate in traffic state i (veh/h); k_i denotes the traffic density in traffic state i (veh/km); v_j denotes the speed of shock wave j (m/s); T_{AC} denotes the time during which the shock wave AC passes through the contraflow lane (s); T_{CE} denotes the time during which the shock wave CE passes through the contraflow lane (s); and h denotes the saturation headway at the main signal (s). The Eq. (7) can be directly used for estimating the optimum length of a contraflow lane given the proposed semi-actuated control strategy, and all the parameters in the Eq. (7) can be measured using field data.

5. Comparison with fixed time CLL design

Simulation experiments were conducted to compare the operational performance associated with the proposed semi-actuated control strategy and those with the fixed time control strategy. The considered CLL design used a conventional and a contraflow lane for discharging left-turning vehicles. Our previous study demonstrated that the CLL design with a conventional and a contraflow lane provided larger capacity for left-turn movement than a conventional left-turn lane did. The contraflow lane served as an extra discharge lane, and the number of left-turning vehicles that was discharged through the contraflow lane can be considered the capacity gains. Theoretically, the maximum capacity gains should be equal to the capacity of a conventional left-turn lane if the contraflow lane was fully used (Wu et al., 2016). In the simulation experiments, the conventional left-turn lane design with dual left-turn lanes was used as a benchmark to identify to what extent the proposed semi-actuated control strategy increased the capacity gains associated with the contraflow lane.

In total, three simulation models were developed, and the characteristics of different design concepts are presented in Table 3. For the CLL design with the proposed semi-actuated control strategy, the distance between the main signal and the upstream median opening (L) was optimized following the procedure provided by the present study, while the L for the CLL design with the fixed time control strategy was optimized following the procedure provided by our previous study (Wu et al., 2016). Note that the L was optimized assuming that the traffic demand during peak periods equaled 550 veh/h, which was the average left-turn traffic demand during peak periods at the selected sites. The simulation models were developed with the software package VISSIM 5.4 based on the geometric design characteristics of one of our selected sites (site 6) and were calibrated and validated based on field data. To evaluate the performance of different design concepts for both peak and off-peak periods, a variety of traffic demand scenarios, which ranged from 300 to 600 veh/h with an interval of 50 veh/h, were considered. For each traffic demand scenario, the results of the first 25 min were omitted to exclude the initiation period of simulation. In addition, the random seeds were changed every 25 min. In total, the simulation ran for 125 min for each scenario. The throughput volume of the left-turning vehicles, the green time for the left-turn movements, and the control delay to the left-turning vehicles were recorded, and the results are shown in Tables 4–6.

The results of the simulation experiments suggest that the proposed semi-actuated control strategy outperforms the fixed time control strategy. As shown in Table 5, the maximum throughput volume of the left-turning vehicles achieved by the semi-actuated control strategy was about 593.8 veh/h, which was slightly smaller than that achieved by the conventional dual left-turn lanes (601 veh/h), but much larger than that achieved by the fixed time control strategy (531.8 veh/h). In all scenarios, the proposed semi-actuated control strategy also generated less delay to the left-turning vehicles than the fixed time control strategy did. In Table 6, t-Test shows that the difference is statistically significant at a 95% level of confidence when the demand is larger than 400 veh/h. When the left-turn traffic demand reached 600 veh/h, the proposed semi-actuated control strategy generated 128.4% less delay to the left-turning vehicles than the conventional fixed-time CLL strategy did. It also should be noted that for the conventional design, a larger demand will always result in a larger delay; however, under low and medium demand, the CLL designs do not necessarily experience a larger delay with increasing demand. This is because the increased demand will promote the use of contraflow lane, lead to a more

Table 3
Characteristics of different design concepts.

Design concepts	Control strategy	L (m)	n_{con}	n_{CLL}	Cycle length(s)
Actuated CLL	Actuated	50	1	1	–
Fixed CLL	Fixed Time	56	1	1	150
Fixed Conventional	Fixed Time	–	2	0	150

Table 4
Average green time for the left-turn movements for different design concepts.

Design concepts	Average green time(s)	Left-turn traffic demand (veh/h)						
		300	350	400	450	500	550	600
Actuated CLL	Main signal	24.2	24.0	24.6	25.6	26.5	27.7	29.3
	Pre-signal	51.3	52.5	56.8	59.8	63.3	66.8	69.6
Fixed CLL	Main signal	30.0	30.0	30.0	30.0	30.0	30.0	30.0
	Pre-signal	45.0	45.0	45.0	45.0	45.0	45.0	45.0
Fixed Conventional	Main signal	30.0	30.0	30.0	30.0	30.0	30.0	30.0

Table 5
Comparison of the throughput volume associated with different design concepts.

Design Concept	Throughput Volume (veh/h)	Demand (veh/h)						
		300	350	400	450	500	550	600
Fixed-CLL	Mean	303.8	340.6	405.6	448.8	499.2	531.4	531.8
	Std. Deviations	74.6	62.7	60.2	69.9	56.2	15.9	15.4
Actuated-CLL	Mean	303.8	352.3	403.7	451.2	499.2	546.2	593.8
	Std. Deviations	81.8	93.5	83.1	98.7	109.7	87.1	67.2
Fixed-Conventional	Mean	303.8	351.4	405.1	449.3	501.6	549.6	601.0
	Std. Deviations	74.0	75.1	77.0	85.2	93.6	87.4	76.6

Table 6
Comparison of delay performance associated with different design concepts.

Design Concept	Delay (s)	Demand (veh/h)						
		300	350	400	450	500	550	600
Fixed-CLL	Mean	62.1	60.7	63.1	68.9	88.6	208.1	223.3
	Std. Deviations	11.1	11.5	12.3	12.9	20.9	40.5	28.6
Actuated-CLL	Mean	60.3	56.8	57.6	55.7	61.0	68.7	130.1
	Std. Deviations	12.1	11.9	10.6	10.4	12.0	20.4	34.9
Fixed-Conventional	Mean	52.0	52.3	53.1	55.9	56.7	57.6	65.1
	Std. Deviations	12.1	12.2	10.0	9.8	8.6	11.4	11.6
P-value of *t*-Test[a]		0.46	0.10	0.01	< 0.01	< 0.01	< 0.01	< 0.01

[a] The *t*-Test of average delay between Fixed-CLL and Actuated-CLL.

balanced queue distribution, and thus decrease average delay. The increasing demand and consequent promotion in the utilization rate of the contraflow lane jointly impact the average delay and result in the non-monotonic relationship between demand and delay, in the low and medium scenarios.

6. Conclusions and discussions

This study proposed a semi-actuated control strategy to improve the operations of the CLL design at signalized intersections. The proposed control strategy introduced an extra stage between the pre-signal and the main signal at the signalized intersection with the CLL design. Two detectors were installed: one at the upstream median opening and the other at the contraflow lanes. A procedure was proposed for optimizing the distance between the upstream median opening and the main signal such that the discharge rate of the left-turning vehicles and the utilization rate of the contraflow lanes can be maximized. Simulation experiments were conducted to compare the operational performance of the proposed semi-actuated control strategy versus the fixed time control strategy. The results show that the proposed design concept outperforms the fixed time control strategy in increasing capacity and reducing delay for left-turning vehicles.

One possible limitation associated with the proposed approach lies in the reliability of the semi-actuated system control system. To address this concern, a backup fixed time control plan can be considered in practical engineering applications. Considering the low utilization rate of contraflow left-turn lanes during low-volume conditions, engineers may also consider closing the contraflow lane during off-peak hours. In addition, numerous factors may affect the performance of the CLL design. One of the interesting issues is the influence of the signal timing of upstream signalized intersections on the operations of the CLL design. The CLL design at different signalized intersections can also be coordinated to maximize system efficiency.

The other possible limitation associated with the CLL design lies in the potential conflicts between the vehicles trapped in the CLL and opposing through vehicles. This condition may happen due to mechanical failure or driver distractions. Even though field data suggest that the chance of vehicles being trapped in the CLL is very small, its potential impacts on safety cannot be fully ignored. With the proposed semi-actuated control strategy, the chance that vehicles are trapped in the CLL is greatly reduced. Thus, the proposed semi-actuated control strategy has potential to increase the safety performance of the CLL design. However, more comprehensive research is needed to evaluate the safety impacts of the CLL design and the proposed semi-actuated control strategy. The authors suggest that future studies should focus on these issues.

Acknowledgements

This research was jointly supported by the National Natural Science Foundation of China (Grant No. 51561135003, 51322810 and 51608268), the Natural Science Foundation of Jiangsu Province (BK20150747) and the Scientific Research Foundation of the Graduate School of Southeast University (Grant No. YBJJ1678). The authors thank the above organizations for supporting this research.

References

Bie, Y., Liu, Z., 2014. Evaluation of a signalized intersection with hook turns under traffic actuated control circumstance. J. Transp. Eng. 141 (5).
Dong, S., Yang, Z., Xu, C., Tian, Z., Liu, P., 2016. Multi-objective evaluation of left-turn waiting areas at signalized intersections in China. Transp. Res. Rec. 2553, 138–149.
El Esawey, M., Sayed, T., 2013. Analysis of unconventional arterial intersection designs (UAIDs): state-of-the-art methodologies and future research directions. Transp. A: Transp. Sci. 9 (10), 860–895.
Guler, S.I., Gayah, V.V., Menendez, M., 2016. Bus priority at signalized intersections with single-lane approaches: a novel pre-signal strategy. Transp. Res. Part C: Emerg. Technol. 63, 51–70.
Hummer, J.E., 1998. Unconventional left-turn alternatives for urban and suburban arterials–Part one. Inst. Transp. Eng. ITE J. 68 (9), 26.
Kozey, P., Xuan, Y., Cassidy, M.J., 2016. A low-cost alternative for higher capacities at four-way signalized intersections. Transp. Res. Part C: Emerg. Technol. 72, 157–167.
Krause, C., Kronpraset, N., Bared, J., Zhang, W., 2014. Operational advantages of dynamic reversible left-lane control of existing signalized diamond interchanges. J. Transp. Eng. 141 (5), 04014091.
Lighthill, Whitham, 1955. On kinematic waves. II. A theory of traffic flow on long crowded roads. Proc. Roy. Soc. London A: Math. Phys. Eng. Sci. 229, 317–345.
Liu, P., Lu, J.J., Hu, F., Socolow, G., 2008. Capacity of U-turn movement at median openings on multilane highways. J. Transp. Eng. 134 (4), 147–154.
Liu, P., Wan, J., Wang, W., Li, Z., 2011. Evaluating the impacts of unconventional outside left-turn lane design on traffic operations at signalized intersections. Transp. Res. Rec. 2257, 62–70.
Liu, P., Yu, H., Wang, W., Ma, J., Wang, S., 2013. Evaluating the effects of signal countdown timers on queue discharge characteristics at signalized intersections in China. Transp. Res. Rec.: J. Transp. Res. Board 2286, 39–48.
Urbanik, T., Tanaka, A., Lozner, B., Lindstrom, E., Lee, K., Quayle, S., Sunkari, S., 2015. Signal timing manual. Transp. Res. Board.
Wong, C.K., Wong, S.C., 2003. Lane-based optimization of signal timings for isolated junctions. Transp. Res. Part B: Methodol. 37 (1), 63–84.
Wu, J., Liu, P., Tian, Z.Z., Xu, C., 2016. Operational analysis of the contraflow left-turn lane design at signalized intersections in China. Transp. Res. Part C: Emerg. Technol. 69, 228–241.
Xuan, Y., Daganzo, C.F., Cassidy, M.J., 2011. Increasing the capacity of signalized intersections with separate left turn phases. Transp. Res. Part B: Methodol. 45 (5), 769–781.
Yang, Z., Liu, P., Wang, W., Ma, J., 2012. Evaluating the operational impacts of left-turn waiting areas at signalized intersections in China. Transp. Res. Rec. 2286, 12–20.
Yang, Z., Liu, P., Tian, Z., Wang, W., 2013. Effects of Left-turn waiting areas on capacity and level-of-service of signalized intersections. ASCE J. Transp. Eng. 139 (11), 1076–1085.
Yang, X., Cheng, Y., 2017. Development of signal optimization models for asymmetric two-leg continuous flow intersections. Transp. Res. Part C: Emerg. Technol. 74, 306–326.
Yang, Q., Shi, Z., 2017. Performance analysis of the phase swap sorting strategy for an isolated intersection. Transp. Res. Part C: Emerg. Technol. 77, 366–388.
Zhao, J., Ma, W., Zhang, H., Yang, X., 2013. Two-step optimization model for dynamic lane assignment at isolated signalized intersections. Transp. Res. Rec.: J. Transp. Res. Board 2355, 39–48.
Zhao, J., Yu, J., Zhou, X., 2018. Saturation flow models of exit lanes for left-turn intersections. J. Transp. Eng., Part A: Syst. 145 (3), 04018090.